Available online at www.sciencedirect.com
SCIENCE DIRECT®
Thermochimica Acta 430 (2005) 73–77
thermochimica acta
www.elsevier.com/locate/tca

Study of the NaBr–$DyBr_3$ phase diagram by differential thermal analysis

D. Kobertz[a], M. Miller[1], U. Niemann[b], L. Singheiser[a], K. Hilpert[a,*]

[a] *Research Center Jülich, Institute for Materials and Processes in Energy Systems, IWV-2, Leo-Brandt Strasse, 52425 Jülich, Germany*
[b] *Philips GmbH, Research Laboratories, Box 500145, 52085 Aachen, Germany*

Received 14 October 2004; received in revised form 10 December 2004; accepted 22 December 2004
Available online 1 February 2005

Abstract

The phase diagram of the quasi binary NaBr–$DyBr_3$ system was determined by differential thermal analysis (DTA) applied to 27 samples covering the complete composition range of the system. The 3NaBr*$DyBr_3$(s) compound is present in the solid-phase in addition to the pure component halides NaBr(s) and $DyBr_3$(s). The $DyBr_3$(s) and 3NaBr*$DyBr_3$(s) phases showed a polymorphic transition at 1112 and at 733 K, respectively. The {$DyBr_3$(s) + 3NaBr*$DyBr_3$(s)} eutectic mixture melts at 709 K giving a liquid of the molar composition x(NaBr) = 0.62. The 3NaBr*$DyBr_3$(s) phase melts peritectically at 765 K. The phase diagram obtained in the present study virtually agrees with the calculated one available in literature.
© 2004 Elsevier B.V. All rights reserved.

Keywords: Phase diagram; Differential thermal analysis; NaBr–$DyBr_3$ system

1. Introduction

Interest in rare earth metal halide containing systems is stimulated by their use as additives in high-pressure metal halide lamps [1,2]. Such lamps are of increasing economic importance due to their luminous efficacy and good color rendering. NaBr and $DyBr_3$ can be important components of the fill in the arc tube of the lamps. As shown by us in a previous study [3], chemical vapor transport of Dy in the NaBr–$DyBr_3$ system is significantly enhanced by the formation of the $NaDyBr_4$(g) hetero complex. The phase diagram of the NaBr–$DyBr_3$ system, the thermodynamic activities of the system components in the condensed phase, and the stability of the vapor species are necessary to predict the vapor composition over condensed NaBr–$DyBr_3$ mixtures of different phases and chemical compositions. We here report on the investigation of the phase diagram of the NaBr–$DyBr_3$ system. The study complements our recent studies on the thermodynamic component activities in the solid phases of the NaBr–$DyBr_3$ system [4] as well as on the thermodynamic modelling [13] and the stability of the vapor species [3] of this system.

While there are thermodynamic and phase diagram studies available for the NaCl–$DyCl_3$ [5,6] and NaI–DyI_3 [7,8] systems in literature, there is no reported experimental phase diagram for the NaBr–$DyBr_3$ system. After completing the present study, Baglio et al. [9] published the NaBr–$DyBr_3$ phase diagram calculated by the multi-species melt model (MSMM). The calculation was based on the enthalpy of mixing estimated from the thermodynamic data for the NaCl–$DyCl_3$ [5,6,10–12] and NaI–DyI_3 [7,8] systems available in literature. The calculated diagram is presented in Fig. 1.

2. Experimental

Twenty-five binary NaBr–$DyBr_3$ samples covering the complete composition range of the system as given in Table 1 were prepared. NaBr(s) (nominal purity 99.999 mass%, Cerac Inc., Milwaukee, USA) and $DyBr_3$(s) (nominal purity

* Corresponding author. Tel.: +49 24 61613280; fax: +49 24 61613699.
E-mail address: k.hilpert@fz-juelich.de (K. Hilpert).
[1] On leave from Wroclaw University of Technology, 50370 Wroclaw, Poland.

0040-6031/$ – see front matter © 2004 Elsevier B.V. All rights reserved.
doi:10.1016/j.tca.2004.12.012

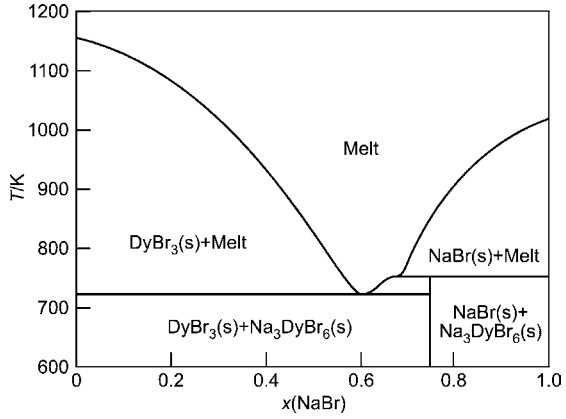

Fig. 1. Calculated phase diagram of the NaBr–$DyBr_3$ system [9].

99.99 mass%, APL, Eng. Mat., USA) were used for the sample preparation. Stoichiometric amounts of the components were melted for 1 h in closed ampoules made of quartz glass and studied subsequently by differential thermal analysis (DTA). The Simultaneous Thermal Analyser, type STA 429, supplied by Netzsch (Selb, Germany) was used in this study. The instrument was interfaced with a Hewlett Packard computer for the automatic recording of the measured signals. The software rendered possible the selection of a particular part of the curve for a detailed scrutiny by varying the sensitivity of the difference signal and the temperature span. The sample weight ranged between 0.9 and 1.3 g. All samples were heated and cooled in a high temperature furnace of the type 6225-03, Netzsch, with heating/cooling rates of 5, 2, and 1 K/min. The heating as well as the cooling schedules for the samples were programmed using the software provided by Netzsch. The software package also included mathematical profiles like Fraser-Suzuki, Cauchy, or Pseudo-Void for peak separation to resolve overlapping peaks of DTA curves. Temperatures were measured with Pt/(Pt + 10%Rh) thermocouples. The thermocouples were calibrated using the following structure change or melting temperatures: 419 °C (Zn), 571 °C (SiO_2), 582 °C (K_2SO_4), 808 °C ($BaCO_3$), 928 °C ($SrCO_3$) and 961 °C (Ag). The SiO_2, K_2SO_4, $BaCO_3$, and $SrCO_3$ samples used in the calibration were from the NBS-ICTA Standard Reference Material 760, supplied by National Bureau of Standards (NBS), now National Institute of Standards and Technology (NIST), Gaithersburg. Each calibration run was carried out by using the three heating/cooling rates of 5, 2 and 1 K/min, the same rates were adjusted for the samples.

Table 1
Mean values of the thermal effects determined in course of the DTA study of the x(NaBr) + (1 − x)$DyBr_3$ samples upon heating (up) and cooling (down) with rates of 5, 2, and 1 K/min

x	Thermal effects[a] (K)							
	Eutectic		Polymorphic		Peritectic		Liquidus	
	Up (n)	Down (n)	Up (n)	Down (n)	Up (n)	Down (n)	Up (n)	Down (n)
0.00			1114.3 (3)	1112.1 (3)			1146.5 (3)	1147.8 (3)
0.05			1114.3 (6)	1107.2 (1)			1139.2 (4)	1138.4 (2)
0.10	708.7 (3)	710.5 (3)					1117.1 (3)	1116.9 (3)
0.20	710.0 (2)	711.4 (3)					1074.1 (3)	1080.8 (3)
0.25	699.1 (2)	703.0 (3)					1018.2 (1)	1018.2 (3)
0.30	708.7 (3)	711.7 (3)					1025.9 (1)	1031.8 (3)
0.40	710.9 (5)	712.7 (3)					986.3 (2)	983.4 (5)
0.50	709.6 (2)	711.7 (1)					885.2 (1)	885.2 (1)
0.55	705.5 (2)	707.1 (3)					793.8 (1)	805.4 (3)
0.60	706.3 (1)	707.0 (3)					–	765.6 (1)
0.62	706.2 (2)	711.2 (2)[b]						
0.64	711.7 (3)	714.9 (2)					712.0 (1)	724.7 (2)
0.65	709.6 (3)	710.1 (4)	–	725.5 (1)[b]				
0.66	706.6 (4)	708.8 (3)	721.1 (1)	722.3 (3)	735.3 (2)	730.4 (2)		
0.68	707.3 (3)	710.4 (4)	734.2 (4)	725.6 (2)				
0.70	711.7 (6)	711.2 (7)	733.5 (5)	726.4 (6)			–	752.8 (3)
0.72	709.1 (2)	707.1 (2)	733.3 (2)	728.6 (2)	–	741.5 (3)	761.0 (2)	761.6 (2)
0.74	708.2 (2)	706.4 (2)	734.8 (2)	729.7 (2)	752.6 (4)	753.9 (5)	769.0 (2)	767.4 (2)
0.75			733.1 (2)	730.2 (3)	761.3 (5)	764.0 (3)	–	773.6 (2)
0.76			733.4 (3)	729.9 (2)	759.6 (3)	765.2 (2)		
0.78			737.0 (2)	734.0 (3)	766.2 (3)	767.3 (3)	822.6 (1)	826.8 (3)
0.80			733.9 (6)	730.3 (9)	763.6 (5)	766.6 (9)	–	854.7 (7)
0.82			736.8 (2)	733.2 (3)	766.3 (3)	767.1 (3)	–	866.6 (1)
0.85			737.6 (2)	733.5 (2)	762.9 (2)	766.7 (2)	911.3 (2)	910.1 (2)
0.87			734.9 (3)	733.4 (3)	761.3 (3)	768.9 (3)	935.1 (2)	930.0 (3)
0.90			735.3 (6)	729.6 (5)	764.3 (7)	769.0 (6)	960.6 (4)	958.4 (6)
1.00							1011.2 (3)	1012.3 (2)

Number of measurements (n) is given in each case.
[a] Estimated absolute accuracy of ±3 K.
[b] The effect can be also assigned to the liquidus temperature.

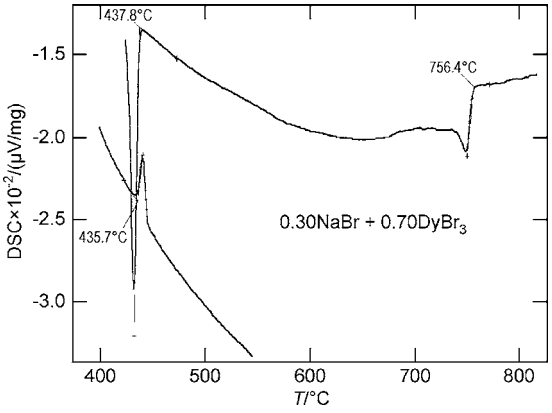

Fig. 2. DTA curve for the sample composition $\{0.30NaBr + 0.70DyBr_3\}$ obtained on heating and on cooling with 2 K/min.

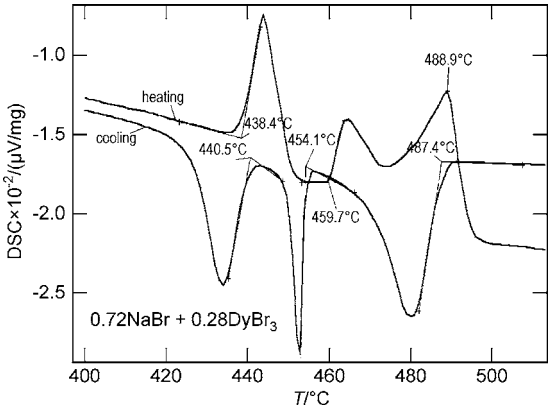

Fig. 4. DTA curve for the sample composition $\{0.72NaBr + 0.28DyBr_3\}$ obtained on heating and on cooling with 2 K/min.

The accuracy of the observed thermal effects was estimated as ±3 K.

3. Results and discussion

Typical DTA graphs recorded for the NaBr–$DyBr_3$ samples with x(NaBr) = 0.30, 0.62, 0.72, 0.75, 0.85 upon heating and cooling with a rate of 2 K/min are exemplified in Figs. 2–6. Though three different heating and cooling rates were employed, the curves recorded only with the cooling rate of 2 K/min were selected for Figs. 2–6. The characteristic onset temperatures of the DTA curves representing phase transitions were evaluated by the determination of the intersection of the extrapolated baseline and the tangents through the inflection point on the leading edge of the peak (onset determination). The DTA curves recorded during the heating and cooling of samples at rates of 5, 2 and 1 K/min were very similar in each case. However, the thermal effects observed on heating of the samples were typically 2–3 K lower as compared to cooling. Table 1 gives the mean value of the thermal effects obtained from several cooling/heating segments for each sample. The assignment of a thermal effect to a phase

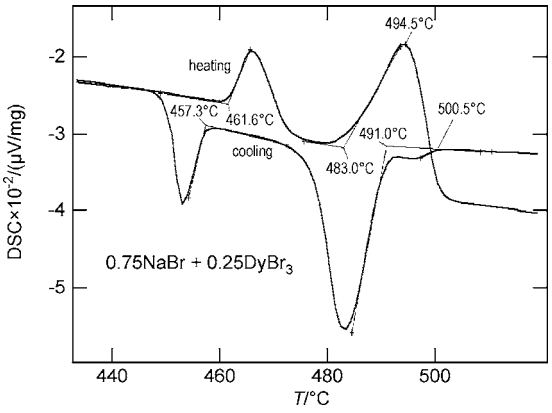

Fig. 5. DTA curve for the sample composition $\{0.75NaBr + 0.25DyBr_3\}$ ('pure' binary compound $3NaBr*DyBr_3$(s)) obtained on heating and on cooling with 2 K/min.

transition was deduced from the shape of the DTA curve, general thermodynamic knowledge, and the known phase diagram of similar systems.

The following general observations were made in the DTA measurements:

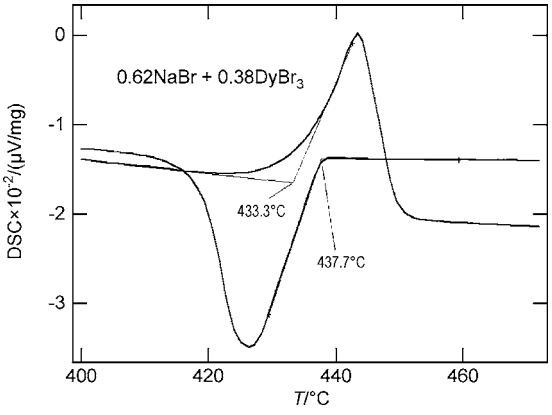

Fig. 3. DTA curve for the sample composition $\{0.62NaBr + 0.38DyBr_3\}$ obtained on heating and on cooling with 2 K/min (eutectic mixture).

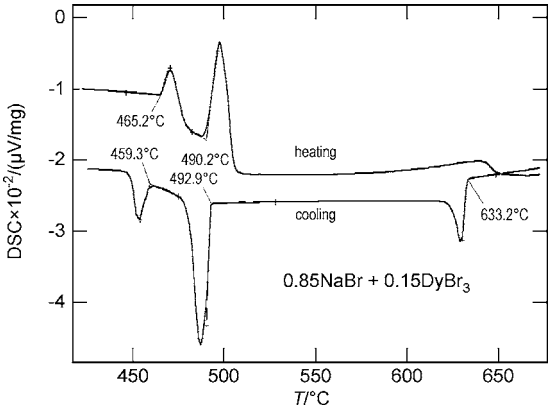

Fig. 6. DTA curve for the sample composition $\{0.85NaBr + 0.15DyBr_3\}$ obtained on heating and on cooling with 2 K/min.

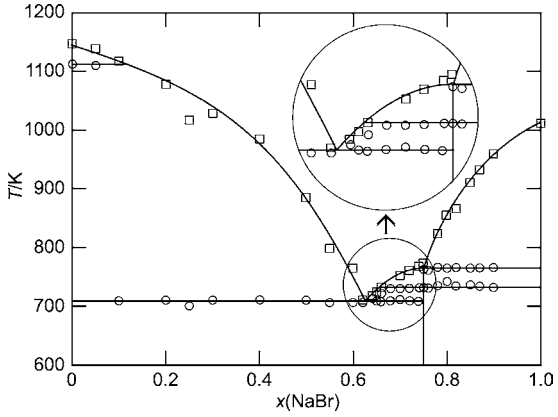

Fig. 7. Thermal effects detected for the samples investigated and phase diagram of the NaBr–$DyBr_3$ system thus obtained.

(a) Samples with $x(NaBr) \leq 0.60$ show two peaks each, one of them (at 709 K) indicates almost the same transition temperature for these samples within the uncertainty of ±3 K (cf. e.g. Fig. 2).
(b) The sample with $x(NaBr) = 0.62$ shows only one strong thermal effect at 709 K which is typical for an eutectic transition (cf. Fig. 3).
(c) Samples with $x(NaBr)$ values between 0.66 and 0.74 show, in general, three phase transitions in the temperature range between 708 and 768 K. Two of them (at 710 and at 730 K) indicate the same temperature for the two samples within the uncertainty of the measurement (cf. Fig. 4). The only exception is the sample with $x(NaBr) = 0.68$ showing only two phase transitions.
(d) The sample with $x(NaBr) = 0.75$, actually being the pure binary compound 3NaBr*$DyBr_3$, shows three phase transitions at 732, 763 and 774 K. The latter gave rise to a very weak signal and could only be registered during cooling with rates of 1 and 2 K/min (cf. Fig. 5).
(e) The sample with $x(NaBr) = 0.76$ shows two thermal effects indicating transition temperatures similar to the two low transition temperatures recorded for the sample with $x(NaBr) = 0.75$.
(f) The samples with $x(NaBr) > 0.76$ show three thermal effects, two of them (at 733 and 765 K) are similar in each case (cf. Fig. 6).

Fig. 7 shows the final phase diagram of the NaBr–$DyBr_3$ system obtained in this study. To simplify the presentation, the mean thermal effects obtained upon cooling and heating are generally given for each sample composition. The only exception is the sample with $x(NaBr) = 0.62$ where the difference between the thermal effects observed upon cooling and heating is larger (5–6 K) as compared to the other samples with differences of ≤3 K. This may be explained by the small difference between liquidus and solidus temperatures giving rise to the observation of the eutectic temperature on heating and of the liquidus temperature on cooling. In spite of this, the eutectic composition was estimated from the diagram in Fig. 7 as $x(NaBr) = 0.62 \pm 0.01$.

The proposed diagram explains all thermal effects identified in the DTA curves in the temperature range of 700–1200 K. The phase diagram shows the existence of the 3NaBr*$DyBr_3$(s) binary phase in addition to the NaBr(s) and $DyBr_3$(s) pure phases. The {$DyBr_3$(s) + 3NaBr*$DyBr_3$(s)} eutectic mixture melts at 709 ± 3 K forming the eutectic melt of the chemical composition $x(NaBr) = 0.62$. It is not quite clear, whether the 3NaBr*$DyBr_3$(s) binary compound melts peritectically or congruently. The weak signal at 763 ± 3 K for the sample $x(NaBr) = 0.75$ suggests rather the peritectic melting of the compound. On the other hand a sample with $x(NaBr) = 0.76$ shows only two phase transitions suggesting the congruent melting of the binary compound with a small deficiency of $DyBr_3$. The composition of liquid at the peritectic temperature is, however, very close (probably even less than 1 mol%) to the composition of the compound. The thermal effect observed at 733 ± 2 K for all samples with $x(NaBr) \geq 0.66$ is evidently a polymorphic transition of the 3NaBr*$DyBr_3$(s) binary compound. No data to this transition are available in the literature so far. The weak thermal effect observed for a sample with $x(NaBr) = 0.65$ at 725.5 K upon cooling can be explained as polymorphic transition of 3NaBr*$DyBr_3$(s) or as liquidus temperature (see Fig. 7).

A comment should be made on the difference of 5 K observed for the postulated polymorphic transition of 3NaBr*$DyBr_3$(s) in the samples with $0.66 \leq x(NaBr) \leq 0.74$ at 729 ± 4 K, in comparison to this transition in samples with $x(NaBr) \geq 0.75$ at 734 ± 2 K. The most probable explanation of this discrepancy is, that the liquid phase present in samples of the composition range $0.66 \leq x(NaBr) \leq 0.74$ in addition to the binary compound improves the thermal conductivity of the sample, thereby decreasing the observed temperatures of phase transitions.

The experimental phase diagram of the NaBr–$DyBr_3$ system determined in the present study agrees very well with that calculated in Ref. [9] by the multi-species melt model (cf. Fig. 1). The eutectic temperature of 722 K and a melt composition of $x(NaBr) \approx 0.6$ are proposed in Ref. [9], which virtually agree with the experimental values of 709 K and $x(NaBr) = 0.62$, respectively, determined in the present study. The 3NaBr*$DyBr_3$(s) binary compound melts peritectically at 753 K according to our investigations unlike Ref. [9]. This also agrees with the respective temperature of 765 K obtained in the present study. The only substantial difference between the phase diagram obtained by us and the diagram calculated in Ref. [9] is the composition of the liquid phase in the peritectic mixture. Moreover, polymorphic transitions were observed in the present study for $DyBr_3$(s) and for the 3NaBr*$DyBr_3$(s) binary compound unlike Ref. [9].

References

[1] D.E. Work, Light Res. Technol. 13 (1981) 143.
[2] K. Hilpert, U. Niemann, Thermochim. Acta 299 (1997) 49.
[3] K. Hilpert, M. Miller, J. Electrochem. Soc. 141 (1994) 2769.

[4] K. Hilpert, M. Miller, J. Alloys Compd. 379 (1/2) (2004) 1.
[5] B.G. Korshunov, D.V. Drobot, Zh. Neorgan. Khim. 10 (1965) 939.
[6] J. Mochinaga, H. Ohtani, K. Denki, Denki Kagaku Oyobi Kogyo Butsuri Kagaku 49 (1981) 19.
[7] J. Kutscher, A. Schneider, Z. Anorg. Allg. Chem. 386 (1971) 38.
[8] J.A. Baglio, C.W. Struck, High temperature materials chemistry, Part II, in: K. Hilpert, F.W. Froben, L. Singheiser (Eds.), Schriften des Forschungszentrums Jülich, Reihe Energietechnik/Energy Technology, vol. 15, Forschungszentrum Jülich GmbH, Central Library, Jülich, Germany, 2000, pp. 719–722.
[9] J.A. Baglio, L.R. Brock, C.W. Struck, Thermochim. Acta 386 (2002) 27.
[10] R. Tagaki, L. Rycerz, M. Gaune-Escard, Electrochemical Society Proceedings of the Ninth International Symposium on Molten Salts, vol. 94, No. 13, 1994, pp. 99–107.
[11] R. Tagaki, L. Rycerz, M. Gaune-Escard, Denki Kagaku 62 (1994) 240.
[12] A.K. Adya, R. Takagu, M. Sakurai, M. Gaune-Escard, Electrochemical Society Proceedings of the 11th International Symposium on Molten Salts, vol. 98, No. 11, 1998, pp. 499–512.
[13] D. Kobertz, K. Hilpert, J. Kapala, M. Miller, CALPHAD 28 (2004) 203.